

Irreversibility temperatures in superconducting oxides: The flux-line-lattice melting, the glass-liquid transition, or the depinning temperatures

Youwen Xu and M. Suenaga

Division of Materials Science, Brookhaven National Laboratory, Upton, New York 11973

(Received 9 August 1990)

The magnetic-field dependence of the irreversibility temperatures follows an $H = a[1 - T_r(H)/T_c(0)]^n$ relationship with $n \cong 1.5$, for pure and alloyed $\text{YBa}_2(\text{Cu}_{1-x}\text{M}_x)_3\text{O}_{7+\delta}$ with $x = 0$ and 0.02 , where $M = \text{Al}, \text{Fe}, \text{Ni},$ and Zn , measured for an applied field parallel to the c axis. However, for $M = \text{Ni}$ and $x = 0.04$ and 0.06 , $n \cong 2.0$. This relationship is not applicable for either $\text{Bi}_2\text{Sr}_2\text{CaCu}_2\text{O}_8$ or $(\text{Bi,Pb})_2\text{Sr}_2\text{Ca}_2\text{Cu}_3\text{O}_{10}$ powders. It is also shown that the irreversibility temperature is a strong function of the magnetic hysteresis width ΔM for pure and alloyed $\text{YBa}_2\text{Cu}_3\text{O}_7$. These results and the measurements of the flux creep $\Delta M(t)$ for these specimens suggest that $T_r(H)$ is a depinning line rather than a lattice melting or glass-to-liquid phase-transition temperature. However, the conventional flux-creep model cannot account for all of the observed temporal dependences of $\Delta M(t)$.

I. INTRODUCTION

One of the most interesting and the technologically important properties of the cuprate high- T_c superconductors, which distinguishes them from those of low- T_c superconductors, is the very weak electronic coupling between the conducting CuO_2 layers,^{1,2} particularly for the Bi and the Tl compounds. This and other related properties of the oxides, such as the short superconducting coherence length ξ (~ 1.5 nm) and large magnetic penetration depth λ (~ 150 nm), result in an unusually high degree of mobility of the magnetic flux lines in these superconductors. This was first noted by Müller *et al.*³ They showed that there is a significant temperature range below the mean-field critical magnetic field $H_{c2}(T)$ in which the magnetization of bulk La-Sr-Cu-O is reversible during a warming and cooling cycle in the magnetic field. The low-temperature boundary of this reversibility range is called the irreversibility temperature $T_r(H)$, which depends on H as

$$H \propto [1 - T_r(H)/T_c(0)]^{3/2}.$$

Based on this and other related observations, they proposed the existence of a superconducting glass state. On the other hand, Yeshurun and Malozemoff,⁴ who observed a similar relationship between $T_r(H)$ and H for a single crystal $\text{YBa}_2\text{Cu}_3\text{O}_7$, argued that this magnetization behavior could be described by a conventional flux-creep model.⁵ Furthermore, they⁴ and Tinkham⁶ derived the same relationship between H and $T_r(H)$ based on a flux-pinning argument.

These highly movable flux lines have also been studied by measurements of the broadening of the resistive superconducting transitions under magnetic fields⁷⁻⁹ and of the complex ac susceptibility near the critical temperatures $T_c(H)$.¹⁰⁻¹² Results of these studies were generally interpreted in terms of the thermally assisted flux motion under the Lorentz force. On the other hand, Gammel

*et al.*¹³ described the observed loss peaks in a $\text{YBa}_2\text{Cu}_3\text{O}_7$ and a $\text{Bi}_2\text{Sr}_2\text{CaCu}_2\text{O}_8$ single crystal as the flux-lattice melting temperature $T_M(H)$ using a high- Q mechanical oscillator. However, Gupta *et al.*¹⁴ concluded that the melting temperature T_M in Ref. 13 was a depinning line based on their comparable data for Bi(2:2:1:2).

These results have also stimulated extensive theoretical studies of the flux motion and the related magnetic phenomena in these materials.¹⁵⁻²³ Noting a drastically reduced tilt modulus of the flux lines due to the high anisotropy in the coherence lengths of these oxides, Nelson¹⁵ predicted, within the context of the anisotropic Ginzburg-Landau (GL) model, the existence of a tangled flux-line phase between the crystalline Abrikosov phase and the mean-field critical magnetic field $H_{c2}(T)$. One of the important assumptions in Nelson's calculation is that the flux lines do not cut across each other. Interestingly, the consequence of this assumption, recently pointed out by Obukov and Rubinstein,¹⁶ is that a flux lattice transforms from a crystalline to a glass state due to topological entanglement of the flux lines and, more importantly, that this glassy phase does not melt until $H \cong H_{c2}(T)$. On the other hand, Brandt¹⁷ and Houghton *et al.*¹⁸ calculated the melting temperatures from the nonlocal elasticity of the flux-line lattice within the anisotropic GL description. In particular, Ref. 18 incorporates the effects of large mass anisotropies^{1,2} and the large GL constant κ in their calculation. Furthermore, they fitted their expression for the melting temperatures, determined by the application of Lindemann's criteria, with the values of $T_M(H)$ from Ref. 13 for $\text{YBa}_2\text{Cu}_3\text{O}_7$ and $\text{Bi}_2\text{Sr}_2\text{CaCu}_2\text{O}_8$ and concluded that $T_M(H)$ is the melting temperature.

In contrast, Fisher¹⁹ recently argued that, in a type-II superconductor with random flux-pinning sites, there exists a disordered phase: a vortex-glass superconductor. [Here it should be noted that this glass state of the flux line is distinctly different from the pinning-induced disordered state of Larkin-Ovchinnikov (LO).²⁴ In the LO model, the long-range order in the flux-line lattice is lost

while, in Fisher's, the short-range coherence is destroyed but order exists at a distance.] Fisher predicted a phase boundary between a vortex-glass (lower temperature) and a vortex-liquid phase (higher temperature) with increasing temperature at a given magnetic field $H (> H_{c1})$, with the irreversibility line being the phase boundary. He also stressed the importance of the random flux-pinning centers in determining the glass-to-liquid transition temperatures, in contrast to other theories for the lattice melting temperatures.¹⁵⁻¹⁸ Subsequently, Fisher *et al.*²⁰ pointed out that this glassy phase is not likely to be stable for $T > 0$ and for high magnetic fields (greater than several kG) in the Bi and the Ti high- T_c oxides. This is due to the fact that the magnetic-flux-line lattice in these highly anisotropic superconductors transforms from a three-dimensional lattice at low fields to a two-dimensional (2D) one at high fields.^{20,21}

Experimentally, following Fisher's work,¹⁹ Koch *et al.*²⁵ showed that the anomaly in the I - V characteristics of a $\text{YBa}_2\text{Cu}_3\text{O}_7$ film as a function of temperature can be interpreted as Fisher's glass-liquid transition. On the other hand, Esquinazi²⁶ argued that Koch *et al.*'s data can be explained by thermally assisted flux flow, and that this vortex-glass-liquid line $T_g(H)$ is equivalent to the depinning line. Furthermore, Inui *et al.*²⁷ demonstrated that the resistive broadening in $\text{Bi}_2\text{Sr}_2\text{CaCu}_2\text{O}_8$ of Palstra *et al.*⁷ can be explained by a single-vortex depinning model. More recently, Griessen²⁸ has shown that Koch *et al.*'s data can be explained by a theory which combines the contributions of the thermally activated motion of the flux lines to the resistivity and of a distribution in energy of the flux-pinning centers. Matsushita *et al.*²⁹ also argued that the irreversibility line is a depinning line in the T - H plane rather than a phase-transition line. On the other hand, Berhuis and Kes³⁰ were able to show that both the flux flow and the lattice melting can exist in an amorphous Nb_3Ge film from the measurements of the resistive transition. Thus, it has not yet been clearly established whether this dissipative magnetic state is a consequence of a phase transformation in the flux-line lattice (or glass) and/or is due to thermally activated motion of flux lines.

In order to gain further understanding and to provide additional information regarding the motion of the flux lines, we have made a series of measurements of the irreversibility temperature $T_r(H)$ for $c \parallel H$ and for a set of c -axis-oriented powders of nominal compositions $\text{YBa}_2\text{Cu}_3\text{O}_7$, $\text{Bi}_2\text{Sr}_2\text{CaCu}_2\text{O}_8$, and $(\text{Bi,Pb})_2\text{Sr}_2\text{Ca}_2\text{Cu}_3\text{O}_{10}$. [Here we refer to these oxides, respectively, as Y(1:2:3), Bi(2:2:1:2), and Bi(2:2:2:3).] We show that $T_r(H)$, as measured by the procedure described below, is similar to the lattice melting temperature $T_M(H)$ determined using the high- Q oscillator¹³ and to the resistive critical temperature $T_R(H)$ obtained with a very low-resistivity criterion (e.g., $\rho = 10^{-4} \mu\Omega \text{ cm}$)⁴⁻⁶. We also studied the influence of substitutional elements on $T_r(H)$ in $\text{YBa}_2(\text{Cu}_{1-x}\text{M}_x)_3\text{O}_7$ (where $M = \text{Al, Fe, Ni, and Zn}$ and $x = 0.02$ except for Ni, $x = 0.02, 0.04, \text{ and } 0.06$) and show that the strength of the flux pinning has a strong effect on $T_r(H)$. Since the measurements of the time-

dependent decay of the critical currents, i.e., $\Delta M(t)$ [$\sim J_c(t)$], at temperatures below $T_r(H)$ can provide a critical test for some of the above models, extensive measurements of $\Delta M(t)$ for these specimens were also made. These results are discussed in detail in terms of the theories describing the motion of the magnetic vortex lines in high- T_c superconductors. Here we only consider the case where the c axis is parallel to the applied field, i.e., $c \parallel H$. (A brief account of this work was reported earlier.³¹)

II. EXPERIMENTAL PROCEDURE

For the purpose of measuring the magnetic-field-dependent irreversibility temperature $T_r(H)$ and critical temperature $T_c(H)$, bulk sintered specimens of the desired compositions were prepared. Detailed descriptions of the preparation methods as well as the results of characterization for superconducting and crystallographic properties and microstructures of these specimens were given previously.³²⁻³⁵ For alignment of the c axis of the powders along the field direction, the specimens were crushed to an average powder size of $\sim 10 \mu\text{m}$ and encapsulated in epoxy under a magnetic field of 80 kG.³⁶ Each capsule contained approximately 100 mg of the powder. The average size of the particle for each specimen was determined by the use of a scanning electron microscope. The alignment was confirmed by transmission Laue and powder x-ray-diffraction techniques.

A commercial SQUID magnetometer (Quantum Design, Inc.) was used for the measurements of magnetic properties. It has been shown that measurements of the magnetic moment of a superconductor in this device require some special precautions.^{37,38} Particularly, overshoots in temperature³⁷ and magnetic field³⁸ must be avoided. Thus, we describe here the exact procedure which was employed for these measurements. Initially, the specimen was cooled to $\sim 5 \text{ K}$ in zero field ($\sim -1 \text{ Oe}$). Then a chosen magnetic-field value was set in several incremental steps. The sample was then slowly warmed to a temperature well above $T_c(H)$ and then slowly field cooled. During a warm-up and cool-down cycle, the temperature was varied by 0.5-K steps for $\sim 15\text{-K}$ spans below $T_c(H)$ and about $T_r(H)$. Between these regions the temperature was changed by 1 or 2 K per step. A thermometer was placed in the specimen chamber of the magnetometer to assure that overshoots did not occur during cycling. However, we observed a small hysteresis in temperature ($\sim 0.1 \text{ K}$) when cycled from low ($\sim 40 \text{ K}$) to high ($> 100 \text{ K}$) and high to low temperatures. This contributes an uncertainty of $\leq 0.25 \text{ K}$ in $T_r(H)$ in this temperature range.

In order to minimize the effects of an inhomogeneous magnetic field (which a specimen has to traverse during the measurement), a 2- or 3-cm scan length was employed, depending on the value of applied field. At these scan lengths, the magnetic homogeneity is better than 2×10^{-5} and 2×10^{-4} for the 2- and 3-cm central region of the superconducting magnet, respectively. At each temperature, three measurements (three scans) were tak-

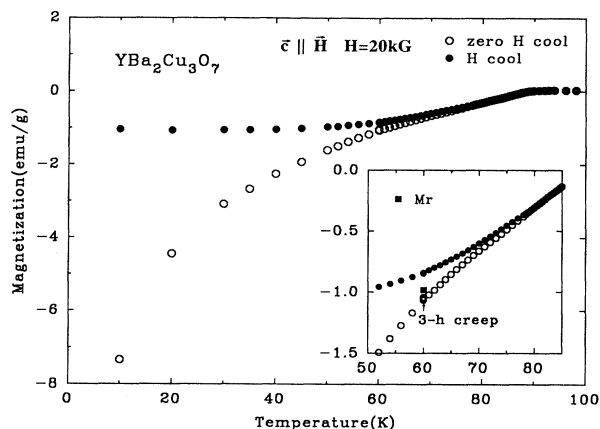


FIG. 1. Magnetic moment vs temperature at $H = 20$ kG for a c -axis-oriented $\text{YBa}_2\text{Cu}_3\text{O}_7$ powder ($c \parallel H$). The inset shows the method used to determine the irreversibility temperature $T_r(H)$ and the change in the moment after $\sim 1.4 \times 10^4$ sec at 60 K. The equilibrium magnetic moment M_R measured from a magnetic hysteresis at 20 kG and 60 K for the same specimen is also shown.

en in the case of a 2-cm scan to improve statistics of the data. Each complete run required ~ 15 – 30 h. These methods were used in order to obtain consistent data, especially in the case of Y(1:2:3). Examples of the results of such measurements are shown in Figs. 1 and 2 for a Y(1:2:3) and a Bi(2:2:1:2), respectively. The insets show the temperature range which includes $T_r(H)$. Two straight lines were drawn from the low-temperature sides,

and the intersection of these was defined as $T_r(H)$. When this criterion was used, the values of the moments at $T_r(H)$ differed by less than $\sim 0.5\%$ for the increasing and decreasing portion of the temperature cycle.

To measure magnetic hysteresis and time decay of the critical current $\Delta M(t)$, we used the procedure which was used earlier to study the flux creep in Y(1:2:3).³⁸ At a given temperature, an applied magnetic field was cycled by small incremental steps, and at predetermined fields the decay in the magnetic moment was also measured up to ~ 3.5 h both on the increasing and the decreasing parts of the cycle. Then $\Delta M(t)$ was calculated by

$$\Delta M(t) = [M^+(t) - M^-(t)],$$

where $M^{+,-}$ are the moments for the increasing and the decreasing portion of the cycled applied fields, respectively. Earlier various magnetic properties of these $\text{YBa}_2(\text{Cu}_{1-x}\text{M}_x)_3\text{O}_{7+\delta}$ were also measured.³⁹ These results are listed in Table I for the use in comparison of the $T_r(H)$ data with the theories.

III. RESULTS AND DISCUSSION

A. The irreversibility temperatures $T_r(H)$ for Y(1:2:3), Bi(2:2:1:2), and Bi(2:2:2:3)

In this section, the values of $T_r(H)$ for Y(1:2:3), Bi(2:2:1:2), and Bi(2:2:2:3) are presented and are compared with the transition temperatures measured by other techniques. Before discussing the results, we will first describe the variations in the magnetic moments as a function of temperature for the shielding and the field-cooling

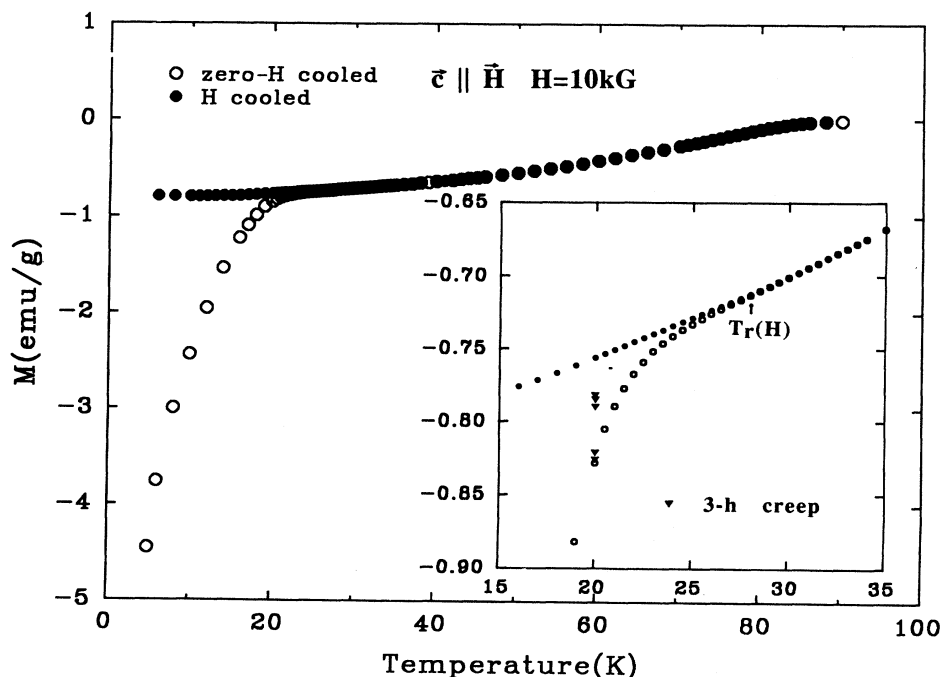


FIG. 2. Magnetic moment vs temperature at $H = 10$ kG for a c -axis-oriented $\text{Bi}_2\text{Sr}_2\text{CaCu}_2\text{O}_8$ powder ($c \parallel H$). The inset indicates the change in the moment with time up to $\sim 1.4 \times 10^4$ sec.

TABLE I. Superconducting properties of $\text{YBa}_2(\text{Cu}_{1-x}\text{M}_x)_3\text{O}_{7+\delta}$.

M^a	T_c (K)	dH_{c2}/dT (kG/K)	dM/dH (emu/cm kG)	$H_{c2}(0)$ (kG)	$H_c(0)$ (kG)	κ	$\xi_{ab}(0)$ (nm)
Cu	90.5	-21	0.0204	1330	17.2	45	1.57
Ni	83.5	-21	0.0115	1230	12.7	57	1.64
0.04	76.3	-23	0.082	1230	11.0	65	1.64
0.06	72.2	-25	0.064	1260	10.0	73	1.62
Zn	68	-21	0.0077	1000	8.8	67	1.82
Fe	86	-19	0.0115	1140	12.3	55	1.70
Al	86	-24	0.0063	1480	11.8	74	1.49

^a $x = 0.02$ except for Ni where $x = 0.02, 0.04,$ and 0.06 .

cycle at very low magnetic field (~ 2 Oe) (see Fig. 3). From the relative values of the shielded to the trapped moments and the sharpness of the transition at $T = T_c$ (2 Oe) for each specimen, one can assess the relative strength of the flux pinning as well as the quality of each specimen. Between the two Bi oxides, one can assume that Bi(2:2:2:3) is more homogeneous and has weaker pinning than Bi(2:2:1:2). Furthermore, the pinning strength in Y(1:2:3) is higher than that in Bi(2:2:1:2) and Bi(2:2:2:3). These observations from Fig. 3 were also confirmed from magnetic hysteresis measurements for these specimens at low temperatures.

The magnetic-field dependence of the irreversibility temperature $T_r(H)$ for a Y(1:2:3) specimen is shown in Fig. 4 in a $\ln(H)$ versus

$$\ln[1 - T_r(H)/T_c(0)]$$

plot. The irreversibility temperature follows a power-law relationship

$$H \cong a [1 - T_r(H)/T_c(0)]^n, \quad (1)$$

where “ a ” is a proportionality constant, and the value of “ n ” is approximately 1.5 as has been observed previously.^{4,10,11} Also shown in Fig. 4 are other transition tem-

peratures determined by various methods; they are (1) the flux-lattice melting temperature T_M (Gammel¹³), (2) the vortex-glass-liquid transition temperature T_g (Koch²⁵), and (3) the resistive transition temperature $T_R(H)$ at $\rho = 10^{-4} \Omega \text{cm}$ for a single crystal (Palstra⁸) and $2.6 \times 10^{-2} \mu\Omega \text{cm}$ for a film (Iye⁹) of $\text{YBa}_2\text{Cu}_3\text{O}_7$. Note that these transition temperatures all follow a similar power-law dependence on H . The values of n for the single-crystal data are ~ 1.5 and for the films, ~ 1.2 . The values of n for single crystals and polycrystals measured here are similar. This suggests that the irreversibility temperatures measured here are comparable to other results for single crystals, as well as films, in providing information about the motion of flux lines. The observed variations in the values of the constants a and n are likely to be due to the variations in sample characteristics, e.g., flux-pinning strength, and in the level of sensitivity of the measurement.

In order to confirm this similarity among the transition temperatures, the magnetic-field dependences of the irreversibility temperatures $T_r(H)$ for Bi(2:2:1:2) and Bi(2:2:2:3) are also compared with T_M^{13} and T_R^7 for Bi(2:2:1:2) single crystals in Fig. 5. For the Bi-based oxides, the relationship between $T_r(H)$ and H does not ex-

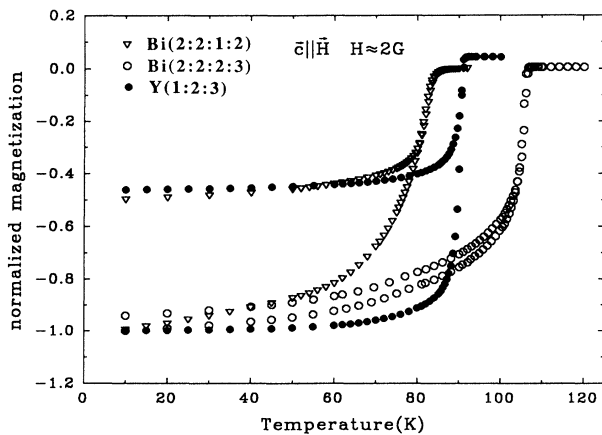


FIG. 3. Magnetic moments for Y(1:2:3), Bi(2:2:1:2), and Bi(2:2:2:3), which are normalized to the zero-field-cooled values, are shown as a function of temperature for a shielding and a field-cooling cycle at $H \cong 2$ G.

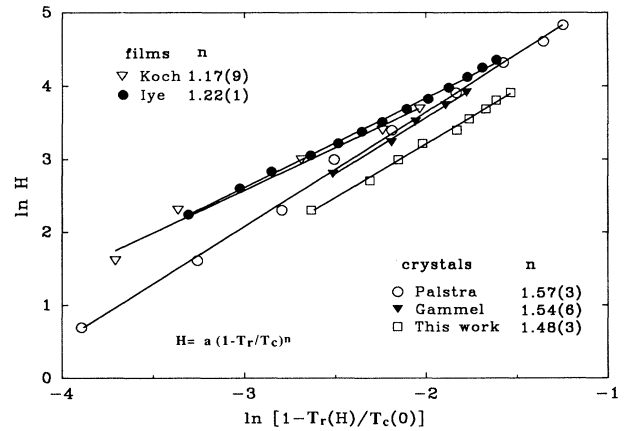


FIG. 4. $\ln[1 - T_r(H)/T_c(0)]$ vs $\ln H$, for a pure $\text{YBa}_2\text{Cu}_3\text{O}_7$ and for other transition temperatures $T_M(H)$ (Ref. 13) (\blacktriangledown), $T_g(H)$ (Ref. 25) (∇), and $T_R(H)$ (Refs. 8 and 9) (\circ , \bullet) described in the text. The numbers in parentheses indicate standard deviations for the last digits in fitting the values of n .

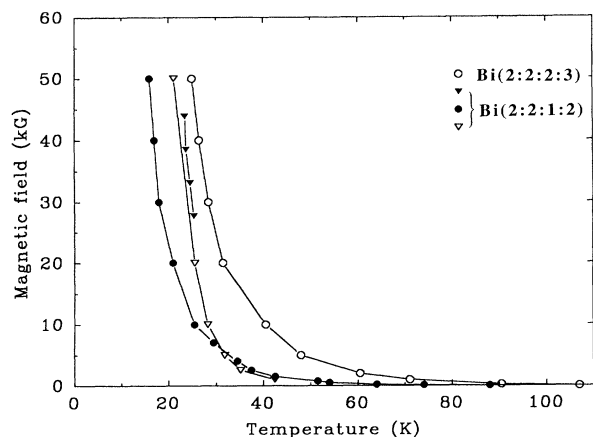


FIG. 5. The irreversibility temperature $T_r(H)$ vs H for $\text{Bi}_2\text{Sr}_2\text{CaCu}_2\text{O}_8$ (\circ) and $(\text{Bi,Pb})_2\text{Sr}_2\text{Ca}_2\text{Cu}_3\text{O}_{10}$ (\bullet) c -axis-oriented powders are compared with $T_M(H)$ (Ref. 13) (\blacktriangledown) and $T_R(H)$ (Ref. 7) at $\rho = 10^{-4}$ m Ω cm (∇).

hibit the same power-law relationship which was found in the Y(1:2:3) system.^{11,40,41} However, the qualitative dependences of these transition temperatures on applied magnetic fields are nearly identical. This is very similar to the situation in Y(1:2:3) although the exact temperatures for T_M , T_R , and T_r are different. Thus, we conclude that $T_r(H)$ as measured here is essentially the same as $T_M(H)$ and $T_R(H)$ and is also likely to be the same as $T_g(H)$, whether these transition temperatures are indications of the lattice melting or the depinning of the flux lines. We also note that $T_R(H)$ for the Bi oxides shown in Fig. 5 does not scale with the values of $T_c(0)$. The difference in $T_R(H)$ between Bi(2:2:1:2) and Bi(2:2:2:3) is approximately $0.05[T_r(H)/T_c(0)]$. Since Bi(2:2:2:3) is a more homogeneous and weakly pinned specimen than Bi(2:2:1:2), based on the results of the magnetic hysteresis and the low-field shielding field-cooling measurements (see Fig. 3), this difference in $T_R(H)$ is thought to be due to the intrinsic difference in these materials, i.e., the number of the CuO_2 layers, two versus three layers in Bi(2:2:1:2) and Bi(2:2:2:3), respectively.

B. Factors influencing the irreversibility temperature

Before discussing whether $T_r(H)$ and other transition temperatures represent vortex-lattice melting, the glass-liquid transition, or the depinning temperatures, we will examine other factors influencing the values of $T_r(H)$ in Y(1:2:3). For this purpose, we have measured the effects due to the substitutions for Cu on $T_r(H)$ and on the strength of flux pinning in Y(1:2:3). The elements Al, Fe, Ni, and Zn were alloyed into Y(1:2:3) to replace 2% of the Cu. For Ni, additional values, $x=0.04$ and 0.06 were also studied. As shown in Fig. 6, the power relationship Eq. (1), between H and $T_r(H)$, was observed for all specimens. For all specimens with $x=0.02$, $n \cong 1.5$ and for $x=0.04$ and 0.06 Ni, $n \cong 2.0$.

Both Fisher's theory on the glass-liquid transition temperatures and the explanation for $T_r(H)$, which is based

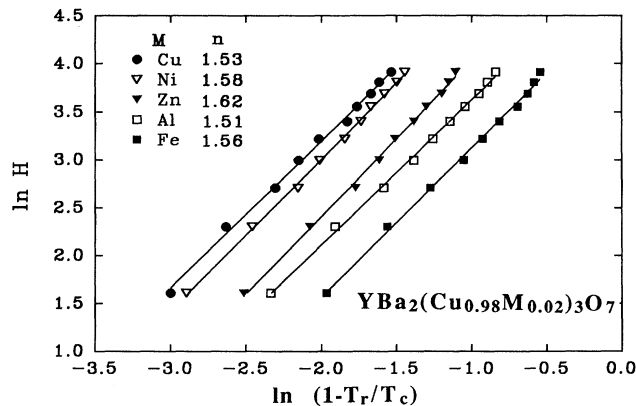


FIG. 6. The irreversibility temperatures $T_r(H)$ for the alloyed specimens, $\text{YBa}_2(\text{Cu}_{1-x}\text{M})_3\text{O}_{7+\delta}$ where $M = \text{Al, Fe, Ni, and Zn}$ and $X = 0.02$ are plotted as $\ln[1 - T_r(H)/T_c(0)]$ vs $\ln H$.

on the thermally activated flux-line depinning, predict that the values of $T_r(H)$, or the constant a , in Eq. (1) are influenced by variations in the pinning strength. We plot a against the pinning strength for each alloy with $n \cong 1.5$ in Fig. 7. Here, the strength of flux pinning is measured by the hysteresis width $\Delta M(T, H)$. $\Delta M(T, H)$ for each alloy was measured at $T \cong 0.1 T_c$ and $T \cong 0.5 T_c$ and $H = 10$ kG. Normalization of ΔM for H_{c2} was not included since the values of H_{c2} are approximately equal for these alloys (shown in Table I). Also, in this plot, the values of ΔM were normalized with respect to small variations in the average size of the aligned powders, i.e., $\Delta M_a = \Delta M d_a / d$, where ΔM and ΔM_a are the hysteresis widths for pure and alloyed 1:2:3, respectively, and d and d_a are corresponding characteristic dimensions. From Fig. 7, it is clear that the pinning strength of a specimen

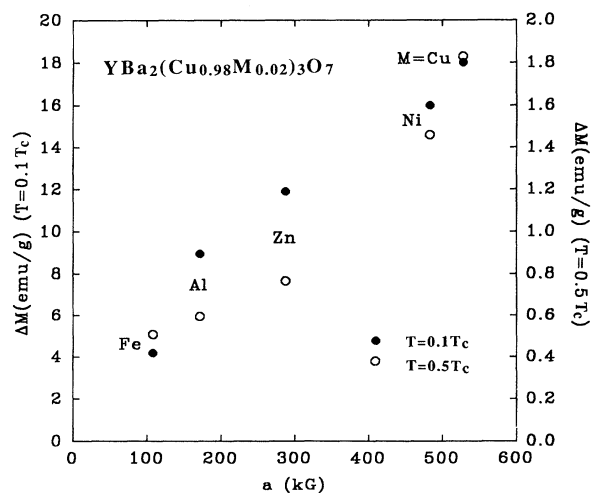


FIG. 7. The effect of variations in the strength of the flux pinning on the irreversibility temperatures is shown by comparing the hysteresis width ΔM at $H = 10$ kG and $T = 0.1$ and $0.5 T_c(0)$ with the proportionality constant a in $H = a [1 - T_r(H)/T_c(0)]^{1.5}$ for pure and alloyed Y(1:2:3).

has a strong correlation with the irreversibility temperature in the case of substituted $\text{YBa}_2\text{Cu}_3\text{O}_7$. In a recent report by Civale *et al.*,⁴² a systematic shift in the constant a in the power law for $T_r(H)$ with increasing ΔM was observed for proton irradiated single crystals of Y(1:2:3). [Note that these authors claimed no variation in $T_r(H)$ after proton irradiation for single crystal Y(1:2:3) in spite of large increases in ΔM . However, if their data is plotted in a log-log plot as in Fig. 4, a consistent increase in a with ΔM is clearly observed. The amount of the observed variation in a is small compared with our present observation. However, this discrepancy is possibly due to the difference in the measurement techniques, i.e., their high-frequency ac versus our dc method.] Furthermore, large increases in the values of $T_r(H)$ associated with the increased hysteresis widths were reported for a neutron-irradiated Bi(2:2:1:2) single crystal⁴¹ and a Tl(2:2:2:3) ceramic specimen.⁴³ Thus, it appears that the observed relationship between the irreversibility temperature and the strength of the flux pinning is a general phenomenon in these superconductors.

Another factor which affects the apparent value of $T_r(H)$ is the rate at which the magnetic field or the temperature is changed during the measurement process. It was reported earlier that the irreversibility temperature is a logarithmic function of the measuring ac frequency in a dc field.^{10,11,44} This frequency dependence was originally described in terms of the depinning rate of the pinned vortex lines in a Y(1:2:3) single crystal.⁴⁴ However, Gammel¹¹ pointed out that, to a certain degree, his similar data for a Bi(2:2:1:2) single crystal can be fit to both the depinning and the glass-liquid transition description for $T_r(H)$.

In the case of dc measurements, we find that $T_r(H)$ also depends on the rate at which temperature is changed. Each temperature step with a 1- or 0.5-K increment required ~ 4 –10 min depending on the temperature range. For the 1-K increment, the average rate of change in temperature is doubled relative to the 0.5-K increment. For 1-K increments, the apparent $T_r(H)$ for Y(1:2:3) is increased 1–2 K higher than for 0.5-K increments. However, as shown in the inset of Fig. 1, when the temperature was held constant for 3 h at 60 K and 20 kG, the moment was reduced by only $\sim 2\%$ of the original value. [This corresponds to $\sim 10\%$ of the difference between the reversible moment M_R and the initial value $M(t_1)$.] In contrast, in the case of Bi(2:2:1:2), if the measurement rate is slowed by holding the temperature for 3 h at a given temperature, e.g., at 20 K, as shown in Fig. 2 (inset), a very significant drop in the magnetic moment is observed. Thus, if a temperature cycle is performed with a 3-h step, a large decrease in $T_r(H)$ could be observed for Bi(2:2:1:2) and Bi(2:2:2:3). However, in the field-cooling cycle, there was no observable change in the moment after 3 h at 60 K for Y(1:2:3) and at 20 K for Bi(2:2:1:2).

These latter observations suggest that slowing the measurement further will not likely appreciably reduce the measured $T_r(H)$. This conclusion conflicts with our interpretation of the creep measurements in the zero-field-cool cycle. Resolving this apparent contradiction will

come with an understanding of the nature of flux motion in these superconductors. A similar observation of no flux creep in the field-cool cycle was made earlier by Müller *et al.*,¹ and this appears to contradict the critical-state model. However, as shown by others,^{37,45,46} a careful study of the flux profile permits this situation within the critical-state model if, at each decreasing temperature step, a flux gradient corresponding to the critical state for that temperature is not established *throughout* the specimen before the next temperature change is initiated, i.e., the magnetic induction gradient in a large central fraction of the specimen is still in the subcritical state for that temperature. Thus, if the temperature is lowered slowly enough below $T_c(H)$ to avoid building the subcritical state field gradient, it appears that a significant reduction in $T_r(H)$ is possible. This also suggests that $T_r(H)$ is a value which depends on the rate and does not have a unique base value which would not be changed by further reduction of the measurement rate.

C. Comparison with theories

At this point, we compare the present results for $T_r(H)$ with the predicted lattice melting temperature $T_M(H)$ of Houghton *et al.*¹⁸ Although Brandt's treatment¹⁷ provides a similar description of $T_M(H)$, Houghton *et al.*'s expression gives an explicit analytical expression for the melting, i.e.,

$$\frac{b^{1/2}}{(1-b)} \left[\frac{4(\sqrt{2}-1)}{(1-b)^{1/2}} + 1 \right] \geq 2\pi E^{-1/2} (M_c/M_{ab})^{-1/2} [(1-t)^{1/2}/t] c^2, \quad (2)$$

where $E = 16\pi^3 \kappa^4 (k_B T_c)^2 / \phi_0 H_{c2}(0)$, $t = T_r(H)/T_c(0)$, $b = H/H_{c2}(T)$,

$$H_{c2}[T/T_c(0)] = H_{c2}^0 [1 - T/T_c(0)],$$

and c is Lindemann's criterion for melting as defined by $\langle u^2(T) \rangle^{1/2} \cong c a_0$. $\langle u^2(T) \rangle^{1/2}$ is the mean-free thermal displacement of a vortex line and a_0 is the flux-line-lattice spacing. c is normally ~ 0.1 for the melting of metals. In order to test the expression, Eq. (2), with our data for $T_r(H)$ for Y(1:2:3) in Fig. 4, we have used the values of T_c , H_{c2} , and κ from Table I and $(M_c/M_{ab})^{1/2} \cong 5$ from the torque measurement.² As is shown in Fig. 8, the best fit was obtained for $c \cong 0.12$ –0.13. This value of c is a factor of ~ 5 smaller than the value which Houghton *et al.* used to fit Gammel *et al.*'s data for Y(1:2:3).¹⁵ The main cause for the difference appears to be their choice of H_{c2} and κ , which were determined from a resistive transition rather than magnetic measurements. Although our value of c is reasonable for Lindemann's criterion, the fit for the entire temperature range is poor and we conclude that the nonlocal elasticity theory for the lattice melting cannot describe the present data nor other data shown in Fig. 4. Attempts to fit Eq. (2), for $T_r(H)$, for Bi(2:2:1:2) and Bi(2:2:2:3) in Fig. 5 were also unsuccessful. These poor fits may be due to one or more of the following possible problems. Our measured $T_r(H)$ [as well as $T_M(H)$,

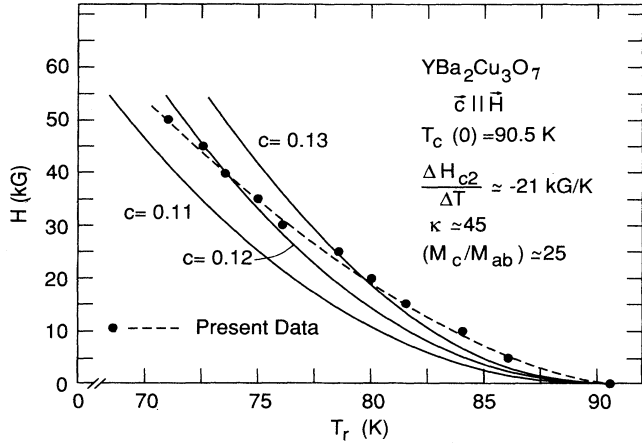


FIG. 8. A comparison of the experimental values of $T_r(H)$ for pure Y(1:2:3) with the theoretical expression (Ref. 18) Eq. (2) for the flux-line-lattice melting temperature for various values of Lindemann's constant.

$T_R(H)$, and $T_g(H)$] may not be the melting temperatures for the flux lattice. These theories do not adequately take into account the effect of flux pinning on lattice dynamics. Or, perhaps, the anisotropic GL model may not be applicable to these oxides.

In contrast, Fisher¹⁹ first pointed out the importance of flux pinning in determining the glass-liquid transition temperature $T_g(H)$. If we assume, following Fisher, that $T_r(H) \cong T_g(H)$, then we see that flux pinning plays an influential role in controlling $T_r(H)$ [shown for the substituted Y(1:2:3) in Fig. 7] as predicted. On the other hand, this strong dependence of $T_r(H)$ on ΔM can also be explained in terms of the depinning model. Similarly, other general observations, which were discussed in Sec. III B cannot be used to decide which of these models is more appropriate in describing the irreversibility temperatures. Thus, it is important to test whether the critical current density $J_c(H, T)$ or the magnetic hysteresis $\Delta M(H, T)$ decays according to the predictions of the glass-liquid transition or the depinning model. The former^{19,20} predicts that

$$J_c(t) \sim \Delta M(t) \sim (\ln t)^{-1/\mu} \quad (3)$$

as $t \rightarrow \infty$ and $\mu \leq 1$. Also, an approximate expression for the intermediate period²⁰

$$J_c(t) \sim \Delta M(t) \sim J_F [1 + (kT/U) \ln(t/t_0)]^{-1/\mu} \quad (4a)$$

and for $\kappa T/U \ll 1$ reduces to

$$J_c(t) \sim \Delta M(t) \sim J_F [1 - (kT/\mu U) \ln(t/t_0)], \quad (4b)$$

where U is the barrier for the vortex-loop excitation, J_F is the nonthermally activated critical current, and t_0 ($\sim 10^{-9}$ sec) is the microscopic attempt time. In contrast, from the thermally activated creep model, one expects⁴⁷ that, for $t \rightarrow \infty$,

$$\Delta M(t) \cong M(0) (2kT/U_c) \exp[-2(t/t_0) e^{-U_c/kT}] \quad (5)$$

and, for intermediate times,

$$\Delta M(t) \cong \Delta M(0) [1 - (kT/U_c) \ln(t/t_0)], \quad (6)$$

where U_c is the pinning potential and $\Delta M(0)$ is the value of ΔM at $T=0$. Here, for simplicity, we will not consider the effect of the deformation of the potential due to the Lorentz force.^{38,48-51} Note that the expressions for $\Delta M(t)$ [Eqs. (4b) and (6)] are identical except for a factor $1/\mu$.

In order to test the veracity of Eqs. (3)–(6), we measured variations in the magnetic moments with time under various conditions for Y(1:2:3), Bi(2:2:1:2), and Bi(2:2:2:3). In the case of Y(1:2:3), two specimens with different powder sizes (~ 10 and $\sim 50 \mu\text{m}$) as well as a textured large-grain specimen (~ 1 mm) were examined. We studied the temperature dependences of ΔM for two temperature regimes: (a) $T \cong T_r(H)$ and (b) $T \ll T_r(H)$. Also, in each temperature regime, we classified the magnetic-field ranges into high and low regions, 10–20 kG and 0.5–3 kG, respectively. The results of the measurements are summarized in Table II according to the functional dependence of the decay in $J_c(t)$ [$\cong \Delta M(t)$]. In each category, the quality of the fit of a function to the data is indicated by the * marks next to the function. No

TABLE II. Temporal functional dependence of $\Delta M(H, T)$ for Y(1:2:3), Bi(2:2:1:2), and Bi(2:2:2:3).

Temperature regime	Magnetic field (kOe)	Specimens and $\Delta M(t)^a$		
		Y(1:2:3)	Bi(2:2:1:2)	Bi(2:2:2:3)
$T \cong T_r(H)$	10,20		$(\ln t)^{-1/\mu}$ *	
		t^{-m} *	t^{-m} *	t^{-m} *
$T \ll T_r(H)$	0.5,1		$\ln t$ *	
			$\ln t + e^{-t}$ *	$\ln t + e^{-t}$
$T \ll T_r(H)$	10,20		t^{-m} **	
	0.5,1,2,3	$\ln t$	$\ln t$	t^{-m} *
			$[1 + (T/U) \ln t]^{-1/\mu}$	$\ln t$ **
			t^{-m} *	

^a The asterisks * next to the functions indicate the degree of the fit; no asterisk, good; *, reasonable; and **, marginal. Those functions, which are not listed indicate that they do not fit at all. $(\ln t + e^{-t})$ indicates the fit for Eqs. (5) and (6).

mark indicates a very good fit, * indicates reasonable, and ** indicates marginal. If a particular functional dependence is not shown in a box, it means that it did not fit at all.

In the regime, $T \cong T_r(H)$, Eq. (3) is applicable since U is expected to be very small at these temperatures. Interestingly, at high fields, 10 and 20 kG, the time decay of the magnetic moments in all specimens was fitted best with a power law, i.e., $\Delta M(t) \propto t^{-m}$ where $m \sim 0.2-0.5$. Although it was possible to force Eq. (3) to fit the data for a large t , the fit was not consistent. Particularly, the condition $\mu \leq 1$ was not always met. However, as previously pointed out,^{20,21} in the case of the Bi oxides, the flux-line system is thought to be a 2D system for $H \geq 3-5$ kG, and, thus, is not expected to obey Eq. (3). Also, somewhat surprisingly, neither the $\ln t$ nor $(\ln t)^{-1/\mu}$ dependence was seen at these temperatures ($T \cong T_r$) for Y(1:2:3) specimens in which a 3D behavior is expected.

In order to investigate the applicability of Fisher's expression, Eq. (3), for the Bi oxides at the fields where a 3D flux-line system is expected, we measured $\Delta M(t)$ near $T_r(H)$ for Bi(2:2:1:2) and Bi(2:2:2:3) at 0.5 and 1 kG. In all cases, however, Griessen *et al.*'s expression for the flux creep, Eqs. (5) and (6), described $\Delta M(t)$ well [shown in Figs. 9(a) and 9(b) for Bi(2:2:2:3) at $T=67$ K and $H=1$ kG, note that $T_r(1 \text{ kG}) \cong 71$ K]. $\Delta M(t) \propto \ln t$ for small t and $\Delta M \propto e^{-t}$ for large t . Thus, under these conditions, $T \cong T_r(H)$ and $H \leq 1$ kG, the flux-line dynamics appears to follow the conventional thermally assisted single flux-line-creep model rather than the glass-state model. Furthermore, using Eq. (6), the value of U_c under these conditions is estimated to be ~ 30 K, which we believe to be a reasonable value.

In the high-field region of the low-temperature regime, $T \ll T_r(H)$, it was observed that the logarithmic dependence of $\Delta M(t)$ was the best fit for both of Y(1:2:3) and Bi(2:2:1:2) (an example is shown in Fig. 10). This logarithmic decay of $\Delta M(t)$ for Y(1:2:3) was reported by others.^{4,38} It is interesting to note that $\Delta M(t)$ for Bi(2:2:1:2) also fit this function even though a 2D magnetic-flux-line system is expected for Bi(2:2:1:2) at these fields. In this region, although a very good fit of ΔM to $\ln t$ was observed, one cannot use this result to distinguish between the two models since Eq. (4b) as well as Eq. (6) predicts approximately the same dependence for $\Delta M(t)$.

At the lower field, as shown in Fig. 11, it is possible to fit the data with Fisher *et al.*'s expression²⁰ Eq. (4a). Here we used $U=200$ K for $H=1$ kG, $t_0=10^{-9}$ sec, and $\mu=\frac{1}{2}$.²⁵ Also, although the value of U is somewhat smaller than that given by Inui *et al.*,²⁷ it is still a reasonable value. Although the fit is not very sensitive with respect to the chosen value of U , it was clearly better with $U=200$ K than with $U=100$ or 400 K. The effects of the variations in t_0 and μ on the fit were not examined. It is interesting to note that the values of U which result in the best fits to $\Delta M(t)$ for Bi(2:2:1:2) and Bi(2:2:2:3) at 3 kG were 100–150 K and 50–75 K, respectively. These values and the trend of U with respect to temperature are also reasonable, as U decreases with increasing field. Also, U for Bi(2:2:2:3) is lower than that for Bi(2:2:1:2), as expected from the width of ΔM at a

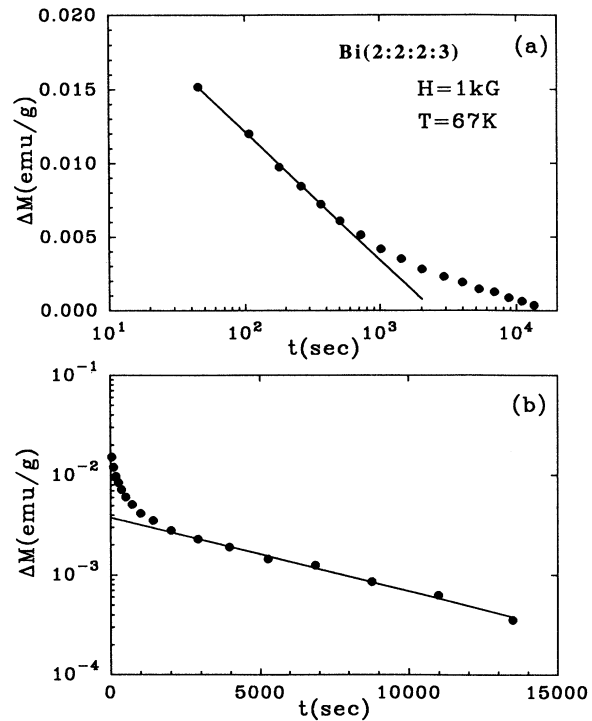


FIG. 9. The temporal dependence of the magnetic hysteresis width $\Delta M(H, T)$ [$\propto J_c(H, T)$] for the Bi(2:2:2:3) at $T \cong T_r(H)$ ($T=67$ K and $H=1$ kG). This is an example in which the prediction by a flux-creep model is followed [Eqs. (5) and (6)]. The same data is plotted in (a) and (b).

similar value of T and H .

In this temperature and field regime, Fisher's model for the temporal dependence of $\Delta M(t)$ [$\sim J_c(t)$] appears to describe the present results quite well. Thus, we will further examine the consequence of Eq. (4a) relative to the temperature dependence of $d\Delta M/d(\ln t)$. As pointed out by Fisher *et al.*, Eq. (4a) leads to a nonmonotonic $d(\Delta M)/d(\ln t)$ with increasing temperature. They cited

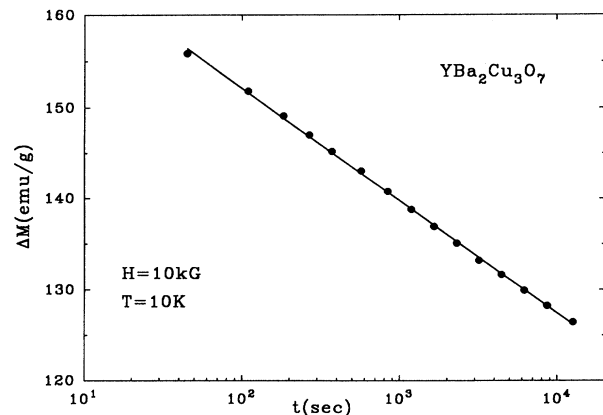


FIG. 10. An example of the temporal dependence of the magnetic moment ΔM for $T \ll T_r(H)$ for a textured Y(1:2:3); $T=10$ K and $H=10$ kG.

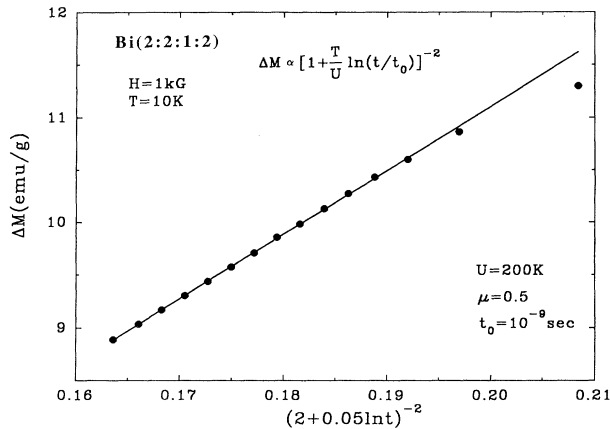


FIG. 11. An example of the temporal dependence of the magnetic moment $\Delta M(H, T)$ for $T \ll T_r(H)$ for Bi(2:2:1:2); $T = 10$ K, $H = 1$ kG, and $T_r(1 \text{ kG}) = 71$ K.

the result from Ref. 4 as evidence for such a nonmonotonic variation of $d(\Delta M)/d(\ln t)$. However, as discussed earlier,³⁸ the maximum in $d(\Delta M)/d(\ln t)$ versus T at high temperatures (~ 30 K) is an artifact due to the choice of the applied magnetic field, which is below the full-penetration field at low temperatures. If the field is applied correctly by cycling to a higher value of H , or $d(\Delta M)/d(\ln t)$ is measured at a higher field, $d(\Delta M)/d(\ln t)$ monotonically decreases above 5 K. As discussed previously,³⁸ this temperature dependence of $d(\Delta M)/d(\ln t)$ is consistent with the idea of a thermally assisted flux motion for the creep. One may expect that the creep rate would increase with increasing temperature, i.e., $e^{-U/kT}$ will increase as kT increases. However, the pinning potential U is a function of ΔM , i.e.,

$$U \cong U_c - (B \nabla B) V X / 4\pi$$

and $\nabla B \sim \Delta M$, where V and X are the activation volume and the width of the barrier. ΔM decreases exponentially with temperature in the material. Thus, the net result is that U/kT increases and $d(\Delta M)/d(\ln t)$ decreases with increasing temperature. Furthermore, it is expected that the rate of the flux motion will be zero at $T=0$ and that there will be a maximum in $d(\Delta M)/d(\ln t)$ as a function of temperature for a thermally assisted flux-motion model. Recently it was shown that this peak is at approximately 3 K for Y(1:2:3) at 2.5 kG.⁵² If we assume this peak is a consequence of Eq. (4a), we find that $U \cong 180$ K using $t = 10^4$ sec and $t_0 = 10^{-9}$ sec. This value of the pinning potential for Y(1:2:3) is thought to be at least an order of magnitude too small. Thus, one concludes that even though the fit of Eq. (4a) to the data of $\Delta M(t)$ for Bi(2:2:1:2) and Bi(2:2:2:3) at $T \ll T_r$ and $H \leq 3$ kG is very good, the model by Fisher *et al.*²⁰ cannot fully describe the motion of the flux lines in these oxides.

There are some difficulties in fitting the data for the temporal dependence of the magnetic moments with the flux-creep model for the entire T and H regimes. But, in general, this picture appears to describe the data better than the glass-liquid transition model. Thus, the present results suggest the $T_r(H)$ lines are the depinning lines in

the T - H plane. The difficulties with both of the models may be possibly related to the fact that they do not take into account the possibility proposed by Brandt²³ that the flux lines cross cut. Hence, more systematic measurements of the temporal dependence of $\Delta M(t)$ as well as theoretical developments for interpretation of $\Delta M(t)$ are required to further our understanding of the irreversibility line $T_r(H)$.

IV. SUMMARY

(1) The irreversibility temperatures $T_r(H)$ for the c -axis aligned powders of pure and alloyed Y(1:2:3) follow $H \sim (1 - T_r/T_c)^n$, and for most cases $n \cong 1.5$. Also, the functional dependence of $T_r(H)$ on H is very similar to that observed for the lattice melting $T_M(H)$, the resistive transition $T_R(H)$, and the irreversibility temperature $T_r(H)$ for single crystals of Y(1:2:3), Bi(2:2:1:2), and Bi(2:2:2:3). This suggests that these temperatures represent the same phenomenon in the flux-line system. Also, due to the similarity between the glass-liquid and the resistive transition temperatures $T_g(H)$ and $T_R(H)$, respectively, for the film of Y(1:2:3), we also suggest that $T_g(H)$ and other transitions are essentially similar measures of the motion of magnetic flux lines in the oxide superconductors.

(2) It was also shown by comparing the magnetic hysteresis width and $T_r(H)$ for pure and alloyed Y(1:2:3) that the strength of flux pinning has a strong influence in determining $T_r(H)$.

(3) The dependences of $T_r(H)$ on H for Y(1:2:3), Bi(2:2:1:2), and Bi(2:2:2:3) were compared with the theoretical expressions for the flux-line-lattice melting temperature. It was concluded that $T_r(H)$ is not the melting temperature of a crystalline flux lattice.

(4) A detailed comparison was made between the temporal decay of magnetic moments $\Delta M(t)$ and the expressions derived for the decay from the glass-liquid transition model and from the depinning line mode of the flux lines. Although the expression for $\Delta M(t)$ from the glass-liquid transition model fit the data very well in a limited temperature and field region, the same expression also led to an unreasonably small value of U for Y(1:2:3). On the other hand, the conventional flux-creep model appears to fit the temporal dependence of $\Delta M(t)$ reasonably well although it cannot describe the present data for all temperatures and magnetic-field regimes. Thus, it suggests that the measured irreversibility temperatures for these oxides are the depinning lines.

ACKNOWLEDGMENTS

The authors acknowledge valuable discussions with D. O. Welch, R. Budhani, and A. R. Moodenbaugh and thank R. Arendt, Y. Gao, and J. E. Crow, and N. D. Spence for providing the Bi(2:2:1:2) and the Bi(2:2:2:3)

powders, respectively. Also, they greatly appreciate D. S. Fisher, M. P. A. Fisher, and D. A. Huse for making their manuscript available prior to its publication. The authors also thank R. L. Sabatini, J. J. Hurst, and F. Perez

for technical assistance. This work was supported by the U.S. Department of Energy, Division of Materials Sciences, Office of Basic Energy Sciences, under Contract No. DE-AC02-76CH00016.

- ¹D. E. Farrell, S. Bonham, J. Foster, V. C. Chang, P. Z. Jiang, K. G. Vandervoort, D. J. Lam, and V. G. Kogan, *Phys. Rev. Lett.* **63**, 782 (1989).
- ²D. E. Farrell, J. R. Rice, D. M. Ginzburg, and J. Z. Liu, *Phys. Rev. Lett.* **64**, 1573 (1990).
- ³K. A. Müller, M. Takashige, and J. G. Bednorz, *Phys. Rev. Lett.* **58**, 1143 (1987).
- ⁴Y. Yeshurun and A. P. Malozemoff, *Phys. Rev. Lett.* **60**, 2202 (1988).
- ⁵P. W. Anderson, *Phys. Rev. Lett.* **9**, 309 (1962); Y. B. Kim, *Rev. Mod. Phys.* **36**, 39 (1964).
- ⁶M. Tinkham, *Phys. Rev. Lett.* **61**, 1658 (1988).
- ⁷T. T. M. Palstra, B. Batlogg, R. B. Van Dover, L. F. Schneemeyer, and J. V. Waszczak, *Phys. Rev. Lett.* **61**, 1662 (1988).
- ⁸T. T. M. Palstra, B. Batlogg, R. B. Van Dover, L. F. Schneemeyer, and J. V. Waszczak, *Appl. Phys. Lett.* **54**, 763 (1989).
- ⁹Y. Iye, S. Nakamura, T. Tamegai, T. Terashima, K. Yamamoto, and Y. Bando, in *High-Temperature Superconductors: Fundamental Properties and Novel Materials Processing*, edited by D. Christen, J. Narayan, and L. Schneemeyer, MRS Symposia Proceedings No. 169 (Material Research Society, Pittsburgh, 1990), p. 871.
- ¹⁰T. K. Worthington, W. J. Gallagher, and T. R. Dinger, *Phys. Rev. Lett.* **59**, 1160 (1987).
- ¹¹P. L. Gammel, *J. Appl. Phys.* **67**, 4676 (1990).
- ¹²P. H. Kes, J. Aarts, J. van der Berg, C. J. van den Beek, and J. A. Mydosh, *Supercond. Sci. Technol.* **1**, 242 (1989).
- ¹³P. L. Gammel, L. F. Schneemeyer, J. V. Waszczak, and D. J. Bishop, *Phys. Rev. Lett.* **61**, 1666 (1988).
- ¹⁴A. Gupta, P. Esquinazi, H. Braun, and H. W. Neuüller, *Phys. Rev. Lett.* **63**, 1869 (1989).
- ¹⁵D. R. Nelson, *Phys. Rev. Lett.* **60**, 1973 (1988); M. Cristina and D. R. Nelson, *ibid.* **41**, 1910 (1990).
- ¹⁶S. P. Obukhov and M. Rubinsten, *Phys. Rev. Lett.* **63**, 1106 (1989).
- ¹⁷E. H. Brandt, *Phys. Rev. Lett.* **63**, 1106 (1989).
- ¹⁸A. Houghton, R. A. Pelcovits, and S. Sudo, *Phys. Rev. B* **40**, 6763 (1989).
- ¹⁹M. P. A. Fisher, *Phys. Rev. Lett.* **62**, 1416 (1989).
- ²⁰D. S. Fisher, M. P. A. Fisher, and D. A. Huse, *Phys. Rev. B* **43**, 130 (1991).
- ²¹S. Doniach, in *High Temperature Superconductivity*, edited by K. S. Bedell (Addison-Wesley, Redwood City, CA, 1990), p. 406.
- ²²N.-C. Yeh, *Phys. Rev. B* **42**, 4850 (1990).
- ²³E. H. Brandt (unpublished).
- ²⁴A. I. Larkin and Yu. N. Ovchinnikov, *Low Temp. Phys.* **43**, 109 (1979).
- ²⁵P. H. Koch, V. Foglietti, W. J. Gallagher, G. Koren, A. Gupta, and M. P. A. Fisher, *Phys. Rev. Lett.* **63**, 1511 (1989).
- ²⁶P. Esquinazi, *Solid State Commun.* **74**, 75 (1990).
- ²⁷M. Inui, P. B. Littlewood, and S. N. Coppersmith, *Phys. Rev. Lett.* **63**, 2421 (1989).
- ²⁸R. Griessen, *Phys. Rev. Lett.* **64**, 1674 (1990).
- ²⁹T. Matsushita, T. Fujiyoshi, K. Toko, and K. Yamafuji, *Appl. Phys. Lett.* **56**, 2039 (1990).
- ³⁰P. Berghuis and P. H. Kes (unpublished).
- ³¹Youwen Xu, M. Suenaga, Y. Gao, J. E. Crow, and N. D. Spencer, *Phys. Rev. B* **42**, 8756 (1990).
- ³²Youwen Xu, M. Suenaga, J. Taftø, R. L. Sabatini, A. R. Moodenbaugh, and P. Zolliker, *Phys. Rev. B* **39**, 6667 (1989).
- ³³Youwen Xu, R. L. Sabatini, A. R. Moodenbaugh, Yimei Zhu, Shin-guang Shyu, M. Suenaga, K. W. Dennis, and R. W. McCallum, *Physica C* **169**, 205 (1990).
- ³⁴R. H. Arendt, M. F. Garbanskas, and L. L. Schilling, *J. Mater. Res.* (to be published).
- ³⁵Y. Gao, J. E. Crow, G. H. Myer, P. Schlottman, J. Schwegler, and N. D. Spencer, *Physica C* **165**, 340 (1990).
- ³⁶D. E. Farrell, B. S. Chandrasekhar, M. R. DeGuire, M. M. Fang, V. K. Kogan, J. R. Clem, and D. K. Finnemore, *Phys. Rev. B* **36**, 4026 (1987).
- ³⁷J. Cave (private communication).
- ³⁸Youwen Xu, M. Suenaga, A. R. Moodenbaugh, and D. O. Welch, *Phys. Rev. B* **40**, 882 (1989).
- ³⁹Youwen Xu, A. R. Moodenbaugh, and M. Suenaga, in *High-Temperature Superconductors: Fundamental Properties and Novel Materials Processing* (Ref. 9), p. 1037.
- ⁴⁰Y. Yamada, S. Murase, K. Yamamoto, and Y. Kamisada, *Cryogenics* **30**, 256 (1990).
- ⁴¹W. Kritschka, F. M. Sauerzopf, H. W. Weber, G. W. Crabtree, Y. C. Yang, and P. Z. Jiang (unpublished).
- ⁴²L. Civale, A. D. Marwick, M. W. McElfresh, A. P. Malozemoff, F. Holtzberg, J. R. Thompson, J. G. Ossandon, and H. A. Deeds, *Phys. Rev. Lett.* **64**, 1164 (1990).
- ⁴³H. K pfer (private communication).
- ⁴⁴A. P. Malozemoff, T. K. Worthington, Y. Yeshurun, F. Holtzberg, and P. H. Kes, *Phys. Rev. B* **38**, 7203 (1988).
- ⁴⁵L. Krusin-Elbaum, A. P. Malozemoff, D. C. Cronemeyer, F. Holtzberg, J. R. Clem, and Zhidong Hao, *J. Appl. Phys.* **67**, 6470 (1990).
- ⁴⁶K. Kitazawa, O. Nakamura, T. Mastushita, Y. Momioka, N. Matohira, M. Murakami, and H. Takei, in *Advances in Superconductivity II*, edited by T. Ishiguro and K. Kajimura (Springer-Verlag, Tokyo, 1990), p. 609.
- ⁴⁷R. Griessen, C. F. J. Flipse, C. W. Hagen, and J. Lensink, *J. Less Common Met.* **151**, 39 (1989).
- ⁴⁸M. R. Beasley, R. Labush, and W. W. Webb, *Phys. Rev.* **181**, 682 (1969).
- ⁴⁹D. O. Welch, M. Suenaga, and Youwen Xu, in *Advances in Superconductivity*, edited by T. Ishiguro and K. Kojima (Springer-Verlag, Tokyo, 1990), p. 655.
- ⁵⁰E. Zeldov, N. M. Amer, G. Koren, A. Gupta, R. J. Gambino, and M. W. McElfresh, *Phys. Rev. Lett.* **62**, 3093 (1989).
- ⁵¹M. P. Maley, J. O. Willis, H. Lessure, and M. E. McHenry, *Phys. Rev. B* **42**, 2639 (1990).
- ⁵²A. Hamzic, L. Fruchter, and I. A. Campbell, *Nature* **345**, 515 (1990).